Adaptive PIV Processing Based on Ensemble Correlation

Christian E. Willert

German Aerospace Center (DLR), Institute of Propulsion Technology, 51170 Cologne, Germany,
e-mail: chris.willert@dlr.de

Abstract The ensemble correlation approach to PIV processing relies on averaging the correlation planes of many images before performing a peak search and subsequent estimation of the average displacement. Generally this processing method has found wide-spread use for the analysis of sparsely seeded micro-PIV image data and can achieve resolution at the single pixel level if the number of images is sufficiently large. The article investigates the potential of the ensemble correlation approach for macroscopic applications driven by two primary motivations: (1) to increase processing speed for the retrieval of mean and fluctuating components, and (2) to provide an estimator to aid in the processing of the individual frames at a later stage.

The ensemble correlation algorithm, implemented as a coarse-to-fine grid refinement approach with adaptive sampling window offset, provides mean velocity data at least one order of magnitude faster than the conventional frame-by-frame PIV interrogation schemes and shows rapid convergence and minimal deviation from averaged data obtained by conventional PIV. Estimates of the fluctuation terms (RMS-values) are derived using a modified peak detection and fitting algorithm based on least squares fitting an elliptically shaped Gaussian distribution.

The method is demonstrated on PIV recordings obtained from a subsonic free air jet and compared to results obtained by conventional (pair-by-pair) PIV processing. Mean displacements are matched within the expected uncertainty of PIV processing except in regions of increased turbulence which exhibit a systematic bias. At this point fluctuating components can only be roughly estimated but can be used the limit the peak search area while the processing of the individual frames at a later stage.

A second example demonstrates the method on PIV recordings obtained from the flow of a transonic compressor. Aside from recovering the mean displacement an order of magnitude faster than conventional PIV processing the sampling resolution could be improved roughly 8 times (32x32 vs. 12x12 pixel) allowing much a higher spatial resolution of compression shocks.

Keywords: PIV, adaptive processing, ensemble correlation, validation, correlation peak

1. Introduction

Without doubt the PIV technique can now be considered a standard flow measurement technique in the field of experimental fluid mechanics, both for fundamental as well as applied research. At this point it is commonplace to acquire ever increasing amounts of image data with inflationary trends very similar to Moore's law for computer hardware. Considerable effort has been devoted to the development of adequate processing algorithms that push spatial resolution and accuracy close to the theoretical limits. Nonetheless numerous tuning parameters are involved to optimize acquisition and subsequent evaluation, such as seeding density, pulse separation, sample size, grid resolution, peak fit, choice of correlation method, validation parameters, image enhancement, etc. The proper choice of many of these parameters can usually only be gained through experience. This makes the quality of a PIV measurement dependent on subjective judgment of the individual user. Thus any tools that are capable of objectively assessing the quality of a PIV measurement are of great value. Ideally these tools should be applicable at the time of image acquisition (e.g., for near real-time adjustment of pulse delay and seeding density) and should provide initial parameters for subsequent processing and validation. Another shortcoming of common algorithms is that most parameters are applied in a global sense, that is, they are constant throughout the field of view while the dynamics

of the examined flow field would call for spatial (or temporal) variation of PIV processing parameters.

The paper explores the possibilities of utilizing the statistical information provided through the analysis of PIV image series (not necessarily time-resolved) on the basis of the so-called ensemble-correlation. Originally introduced by Wereley et al. [1] for the evaluation of micro-PIV data to overcome effects due to Brownian motion and increase spatial resolution in spite of sparse seeding, it has received little attention for its possible use in classical macroscopic PIV applications. The main concept behind ensemble correlation is to average cross-correlation planes over many images rather than averaging the extracted displacement vectors. The mean displacement is then obtained from the average correlation planes whose correlation peaks typically have a considerably larger signal-to-noise ratio than the correlation peaks in the correlation data obtained from the individual image pairs. If the image number is large enough even single pixel spatial resolution can be achieved [2][3].

One great advantage of ensemble-correlation is that the mean displacement field can be obtained considerably faster than by using conventional image-by-image analysis. This can be exploited to rapidly assess PIV image quality as well as provide initial estimates for evaluation of the individual image pairs. As illustrated in Fig. 3 the shape of the averaged correlation peak contains additional information that can be related to the statistical variation of the displacement. This property was initially utilized by Hohreiter et al. [4] to estimate temperature in micro-PIV as the Brownian motion of the particles is a function of temperature. A more detailed analysis of the contributing factors in correlation peak formation was performed by Kähler & Scholz [3] and applied in a long-distance micro-PIV setup.

The class of proposed algorithms suggested here uses ensemble correlation on a given PIV image series to recover the mean displacement and in addition evaluates the averaged correlation peak shape to extract detection bounds for processing the individual PIV image pairs (see Fig. 6 and Fig. 5). The algorithms inherently offer the capability of spatially varying detection criteria. Further, each individual search mask may be combined with its own weighting function based on the averaged correlation peak shape which provides an additional validation criterion (e.g. likelihood of valid vector) as illustrated in Fig. 7.
The paper examines the performance and potential of the algorithms on PIV data sets from several experiments.

2. Implementation

On the whole the ensemble correlation approach is a rather simple technique to implement by extending standard PIV algorithms. Rather than processing each image pair individually, the correlation plane data obtained for each sampling position is stored and accumulated while processing a multitude of images. This is outlined in Fig. 1 for a single sampling position. After interrogating all images the displacement information is extracted from the averaged correlation planes employing the established peak detection and sub-pixel fitting schemes available from conventional PIV processing.

Fig. 1 also nicely illustrates one of the primary advantages of the ensemble correlation approach: random noise present in the individual correlation planes is drastically reduced in the averaged correlation plane. This favorable behavior can also be taken advantage of when interrogating single image pairs as demonstrated by the correlation-based-correction technique introduced by Hart [5]. In that case a multiplication of correlation planes was chosen to eliminate spurious correlation signals, but at the same time has the disadvantage that a single uncorrelated plane causes a complete loss of signal. Because of this summation of correlation is favored for the analysis of image sequences [1]. The addition has the advantage that uncorrelated images (e.g. due to image acquisition problems, low seeding) have no negative impact on the cumulative average of the correlation.

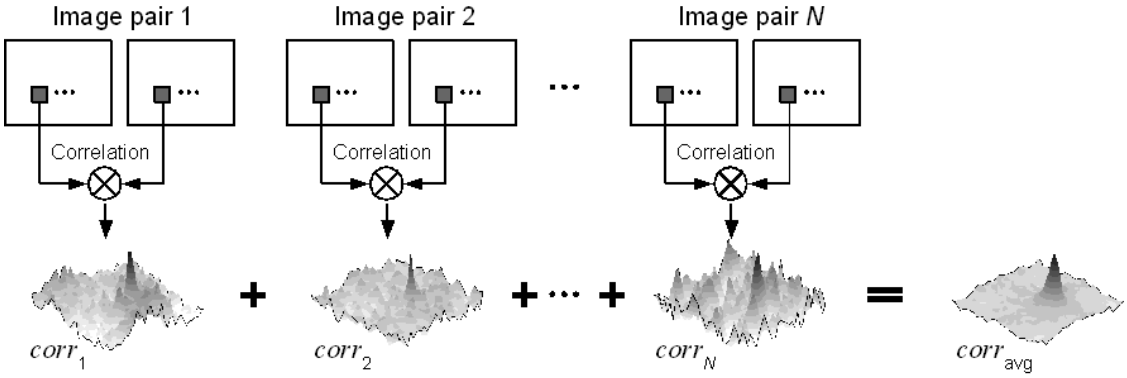

Fig. 1: Basic approach for creating the ensemble-averaged cross-correlation plane using a sequence of PIV image pairs

2.1 Adaptive ensemble correlation

The previously outlined processing approach lends itself to adaptive processing approaches that are commonly implemented in conventional PIV analysis. Displacement data obtained in earlier interrogation passes is used as a predictor for the next interrogation pass which increases the signal detection rate (due to improved particle matching) and allows a gradual decrease of the sampling window thus increasing the spatial resolution. The discrete window offset, proposed by Westerweel et al. [6] can be applied here in the exact same manner, with the minor difference that the local window offset is common for all images of the sequence.

The second important adaptive feature of the proposed ensemble correlation algorithm is the use of a coarse-to-fine processing pyramid similar to the adaptive scheme used in conventional PIV analysis as implemented by Willert [7]. Just as in the implementation for standard PIV, image down-sampling by summation of $N \times N$ pixels is used to reduce the image size and allow fast processing using small sampling windows. Due to the rapid convergence of the ensemble correlation approach a reduced number of images can be used at the coarser resolutions which further increases processing speed. Additional enhancements can be achieved by using summation property of the Fourier transform as described in Appendix A.1. The code also is well suited for parallel implementation such that further speed increases are only limited by the transfer rate of images from storage device into memory.

Table 1 along with Fig. 2 give an example of the described coarse-to-fine processing scheme using a sequence of 100 image pairs with a depth of 16 bits/pixel and a resolution of 1200×768 pixel. On an Intel 3 GHz Pentium 4 (1 GB RAM) processing took 85 seconds. The first two iterations given in the Table 1 clearly demonstrate that reliable displacement estimates can be extracted using only a small number of images (10-20). Of course a nearly stationary flow is required to achieve this sort of convergence. Nonetheless good displacement estimates can be extracted in the highly turbulent shear layer region – partially also because the sampled images are uncorrelated (randomly sampled).

Table 1: Example of coarse-to-fine multi-grid approach for adaptive ensemble correlation (all dimensions in pixels)

Interrogation step	1	2	3	4
Sampled images	11 of 100 (9%)	25 of 100 (25%)	50 of 100 (50%)	100 of 100 (100%)
Desampled image size	400 x 256	600 x 384	1200 x 768	1200 x 768
Sample size	32 x 32	32 x 32	32 x 32	24 x 24
Eff. sample size	96 x 96	64 x 64	32 x 32	24 x 24
Overlap	0%	0%	0%	50%
Image size				

No. of vectors	12 x 7 = 84	19 x 11 = 209	39 x 23 = 897	105 x 63 = 6615

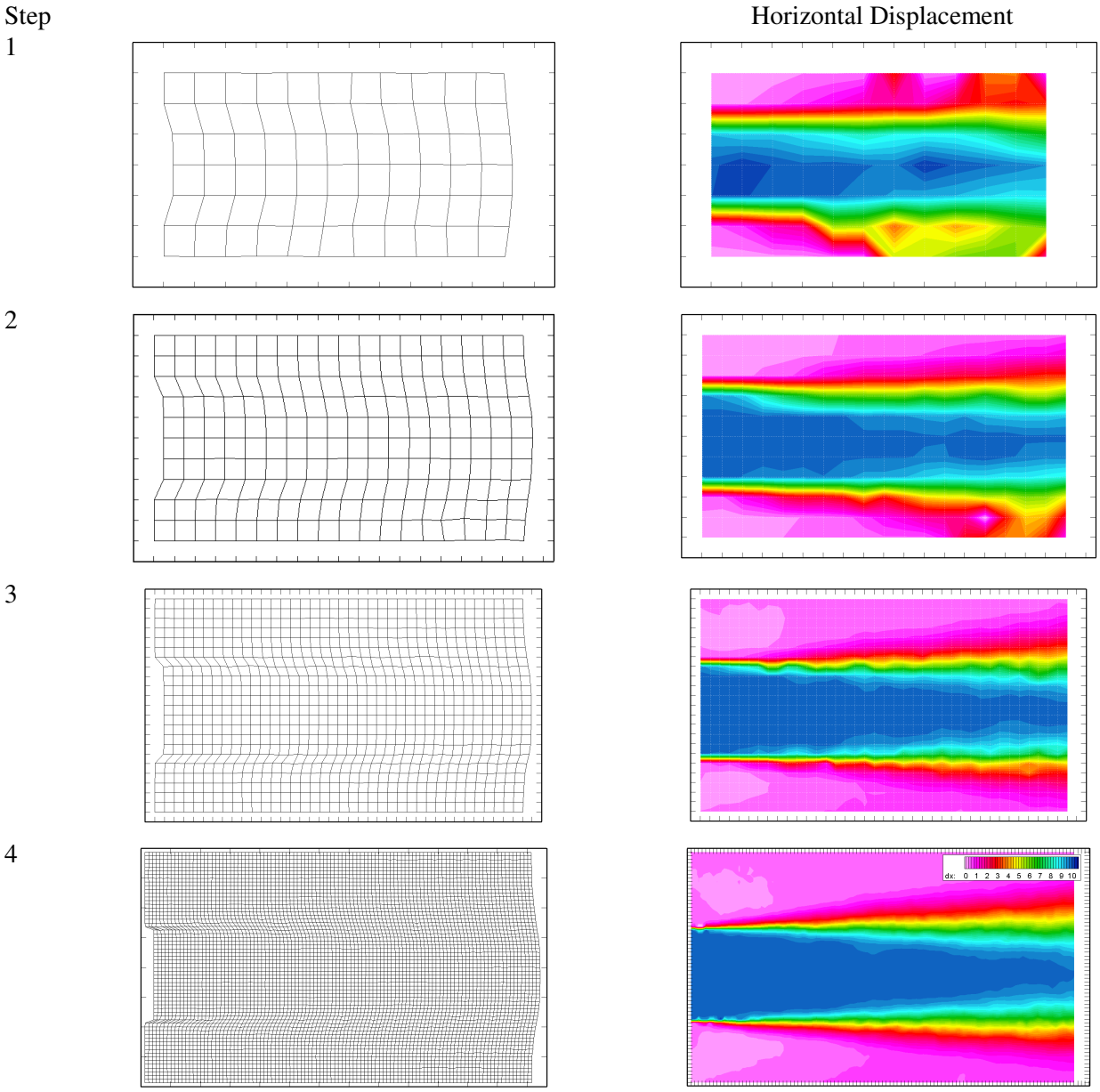

Fig. 2: Distorted sampling grid (left) and horizontal displacement component (right) for coarse-to-fine interrogation given in Table 1

2.2 Correlation peak detection and shape estimation

In principle the same correlation peak detection scheme as for conventional PIV can be used for the analysis of the average correlation maps. A Gaussian fit in two-dimensions is on 5 or 9 points is sufficient. However, the correlation peak broadens as the velocity fluctuation in the sampled area increases. This is illustrated in Fig. 3 and for actual ensemble-processed PIV recordings in Fig. 4. Contrary to conventional processing peak detection and fitting of the average correlation plane data needs to account for two additional aspects: the baseline of the correlation peak is not necessarily zero due to the accumulation of noise and the shift of the individual peaks around a mean position. Second, the shape of the correlation peak depends on the underlying flow statistics. The plots provided in the second row of Fig. 4 show a strongly distorted correlation peak obtained it the shear layer region of a free air jet. Its shape is roughly elliptical with its major axis rotated with respect to the frame of reference. This rotation reflects the fact that the statistical variation of the

displacements u' and v' are correlated, that is, the Reynolds stress term u'v' is non-zero. While this is only of marginal importance for the estimation of the mean displacement from the maximum of the peak any further estimation of correlation peak widths needs to account for this rotation. Appendix A.2 outlines how the rotation can be incorporated in a Gaussian peak fit.

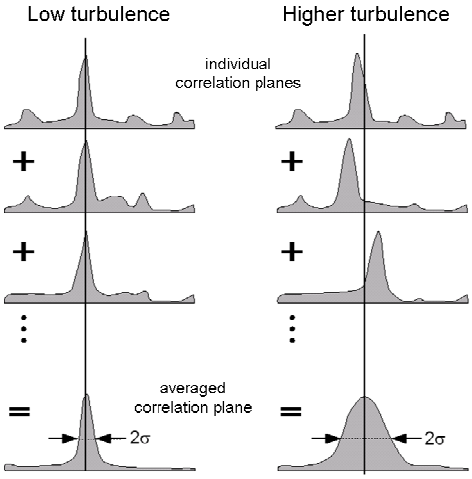

Fig. 3 Effect of varying displacements on correlation data and on mean correlation peak shape

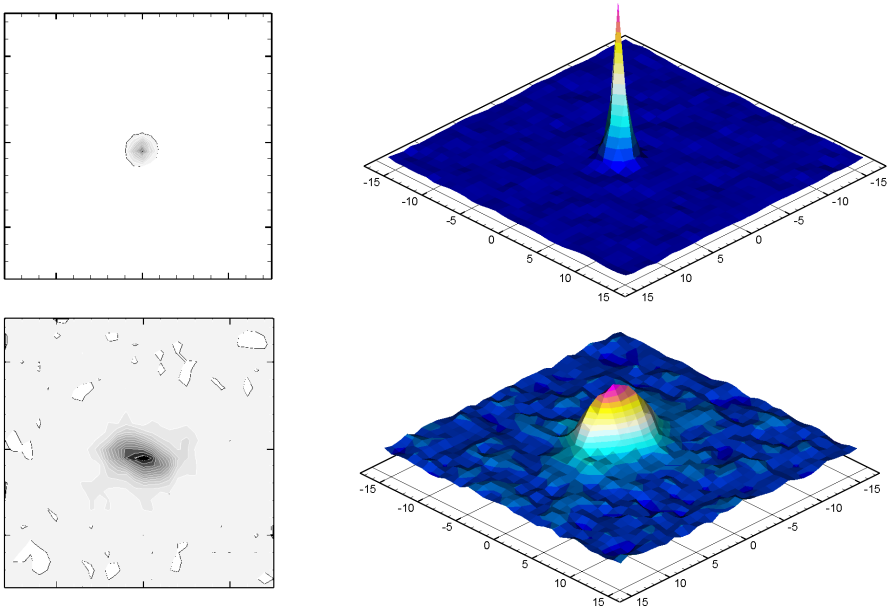

Fig. 4 Top row: cross-correlation peak obtained in uniform jet core flow, bottom row: peak broadening due to flow turbulence in lower shear layer of free jet

As indicated before, the fluctuating components u' and v' are contained in the correlation peak shape. Using the theoretical description of PIV cross-correlation (e.g. Adrian [8] or Westerweel [9]), the correlation signal for standard double-frame PIV can be decomposed of a so-called displacement correlation peak, a constant background correlation term and the correlation between the mean and the fluctuating components. The width of the displacement correlation peak reflects the mean particle image shape (e.g. diameter) and is broadened by the variation of particle image displacements within the sampled area. If the particle image diameter can be properly accounted for then the remaining width of the correlation is a measure of the displacement fluctuation within the sampled area. To first order this can be estimated by subtracting the width of the autocorrelation peak (i.e. the mean particle image diameter) from the cross-correlation peak width. This approach is extended to ensemble-averaged correlation in order to estimate the

fluctuating displacement (velocity) components of the image sequence. Clearly, this is a rather crude approach and likely ignores some additional statistical terms arising through the summation of many correlation planes. A discussion of how the fluctuating terms enter in ensemble-correlation is given by Kähler & Scholz [3]. They conclude that the cross-correlation peak width can only be related to the flow turbulence in the case of isotropic turbulence. For the more common non-isotropic turbulent flows the correlation peak width can merely provide estimates, as will be demonstrated later.

Because of the wide range of possible correlation peak shapes, the peak detection and fitting is implemented in a two step procedure. First a blob analysis extracts contiguous pixels that exceed a certain threshold, derived from the mean correlation C_{avg} and its standard deviation C_{rms}: $C_{thr} = C_{avg} + c_o \cdot C_{rms}$ with the constant c_o in the range of 1-3. In the second step the pixel region with the highest correlation vlaues is fitted to a Gaussian intensity distribution using a non-linear Levenberg-Marquardt least squares approach [10]. In total 7 parameters are minimized: the position of the correlation peak $[x_o,y_o]$, its width with respect to the major axes σ_x, σ_y, the peak amplitude A, the base-line C_o and a skewness factor k accounting for the rotation of the ellipse shaped correlation peak (see Appendix A2). A simplified fit is also performed on the averaged autocorrelation data, excluding the factors k and C_o. The fluctuating terms of the displacement (i.e. u' v') are then estimated by subtracting the autocorrelation peak widths from the estimated cross-correlation peak widths.

2.3 Subsequent PIV processing of the unsteady data

The average displacement map along with the recovered correlation peak widths is well suited as a predictor for subsequent analysis of the individual image pairs as illustrated in Fig. 5. In particular, three parts of information are used to guide the PIV processing:

1. The local displacement is used to offset the correlation samples with respect to each other, or to deform the images just as in advanced iterative multi-pass schemes thereby accounting for the average displacement. This reduces the number of number iterations and allows the use of small sampling windows right from the beginning.
2. The previously determined dimensions of the ensemble-averaged correlation peak define a search area for the correlation peak during pair-by-pair processing (Fig. 6).
3. The shape of the average correlation peak (amplitude distribution) can be used to weight the recovered correlation signal. Here it can be assumed that a correlation peak with low weight will have a greater likelihood of being a false measurement (Fig. 7).

The last two features are rather unique in PIV processing because they introduce spatially varying validation criteria. More uniform flow regimes have narrower correlation peaks and hence more stringent peak detection bounds, whereas turbulent zones automatically allow for wider peak detection bounds.

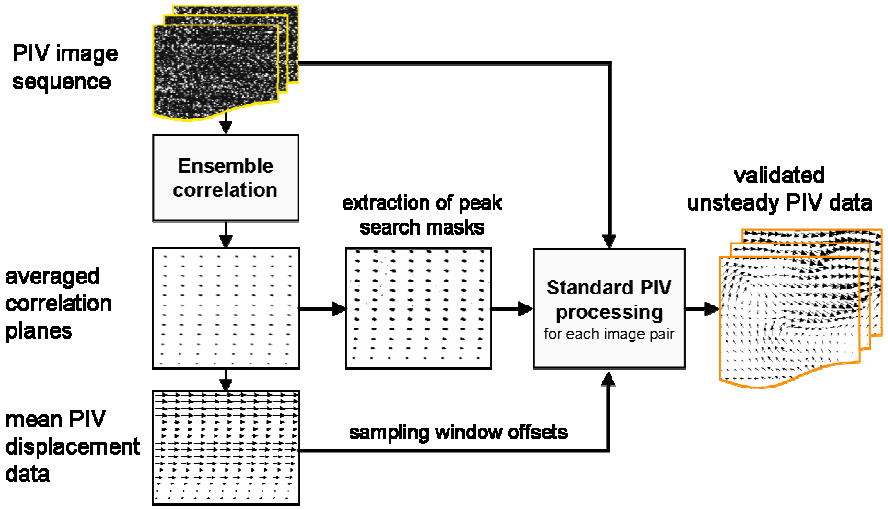

Fig. 5 Proposed PIV processing algorithm with spatially varying correlation peak detection criteria

3. Performance tests on actual PIV data

3.1 Free jet

The sample data shown in Fig. 2 were obtained for a subsonic air jet (d = 20 mm nozzle, $U_o \approx 66$ m/s, $Re_d = 82500$) issuing into quiescent and partially unseeded air. One hundred images were used for ensemble averaging. The displacement data recovered through ensemble correlation is compared to averaged results obtained with conventional multi-grid PIV processing. The map of displacement differences between the two averaged data sets is shown in Fig. 8 and exhibits some noteworthy artifacts: the jet core flow and the exterior quiescent region have minimal deviations of less than 0.05 pixel which corresponds to the expected uncertainty of PIV at this sampling area (32x32 pixel). On the other hand the shear layer regions show systematic deviations of up to 0.5 pixel. Near the jet's potential core, the average displacement within the shear layer is overestimated by the ensemble correlation method while the exterior region is underestimated. This bias effect is most likely introduced because certain statistics introduced during averaging of correlation planes are not accounted for. It should be noted that these artifacts are not related to peak locking.

Large displacement deviations are present near the jet's nozzle and result from the bi-modal velocity distribution within the local sampling volume: both high-speed jet flow and quiescent exterior flow are sampled simultaneously – the spatial resolution is insufficient here. While standard PIV processing statistically averages the results of both velocities over many images, the ensemble correlation method accumulates a correlation plane with two distinct correlation peaks of which the peak detection scheme uses only the strongest. These two peaks are very clearly discernable in Fig. 9 where the left peak corresponds to the nearly quiescent jet entrainment flow, the right peak is associated with the high speed jet flow; the separation between these peaks is about 10 pixels.

3.2 Transonic Compressor

A more challenging performance test for the ensemble-correlation approach is PIV image data obtained from a transonic compressor facility. In particular the project studied the flow in the vicinity of so-called *casing treatments* was investigated and compared to CFD results. Casing treatment is known to improve the performance envelope of compressors but the mechanisms are not fully understood. Further details about the project background, the PIV measurements and comparisons to CFD can be found in [11]-[13].

Here the ensemble-correlation method is applied on image data acquired at 87% blade height while the compressor was operating at peak efficiency. In total 204 image pairs (1 GB) were processed within 5 minutes whereas conventional pair-wise processing required 1h:30min using multi-grid processing combined with iterative image deformation. The recovered average velocity data matches very well between the two averaging approaches, with slightly more noise in the result

of the ensemble correlation approach (Fig. 11 and Fig. 12). Since the flow conditions were essentially stationary, the spatial resolution could be increased using the ensemble-correlation approach. Whereas standard PIV sampled the flow at 32x32 pixel (1x1 mm^2) the sampling window could be reduced down 12x12 pixel (0.3x0.3 mm^2) for ensemble-correlation. This is made possible by the iterative coarse-to-fine sampling approach combined with discrete window shifting of the ensemble-correlation method. A further reduction of the sampling area is principally possible but makes little sense here because the mean displacement of the oncoming flow already is on the order of 10 pixels. Also the velocity lag of the particles will become increasingly dominant. The advantage of the increased spatial resolution is that certain features in the flow can be resolved much better. As shown in Fig. 13 the compression shock upstream of the compressor blade exhibits a much sharper transition from high-speed to low-speed flow. The spatial width of this transition could be reduced from about 1.2 mm down to 0.5 mm. This is close to the mean displacement of particle images (10-12 pixel) which combined with the particle lag is the best achievable resolution of the compression shock under these imaging conditions.

4. Conclusions

The paper demonstrated the potential of the ensemble correlation approach for use in macroscopic flows commonly found in applied aerodynamics, turbomachinery and related areas where statistical quantities such as mean velocity and fluctuations are of primary interest. The method, implemented in a coarse-to-fine grid refinement approach with adaptive sampling window offset, provides mean velocity data at least one order of magnitude faster than the conventional frame-by-frame PIV interrogation schemes and shows rapid convergence and minimal deviation to averaged data obtained by conventional PIV. Also, it was found that contrast enhancing image processing prior to correlation processing is not as important as in conventional PIV processing were it is frequently used.

The recovered mean displacement data also serves as a reliable initial estimate for subsequent processing of the individual PIV recordings, with the previously recovered correlation peak widths serving as detection bounds and weighting factor for the correlation signal detection step.

Through proper analysis of the averaged correlation planes further statistical data such as the RMS values of the velocity (displacements) can be estimated. A first order approach was suggested here and relies on subtracting the width of the autocorrelation peak from the width of the cross-correlation peak. A general underestimation of the RMS values with respect to conventionally processed PIV data was observed. Clearly further investigations are necessary to properly recover the information from the correlation distribution, especially to properly account for mixed terms that rotate the major axis of the elliptic correlation peak.

The ensemble correlation approach was also applied for the accurate measurement of volume flow through a pipe using a stereoscopic imaging arrangement [14]. In this case the back-projected images from each view were first processed by the ensemble correlation approach, followed by the stereoscopic reconstruction of the average three-component velocity field. This approach contradicts common practice where the reconstruction precedes the averaging step to avoid possible velocity biasing. In the present case the orthogonal imaging arrangement meant that the projected velocity components observed by each camera and responsible for the reconstruction of the out-of-plane component were practically orthogonal to each other and thus did not contribute to possible bias effects.

So far the performance of the proposed ensemble-correlation method has only been studied using real PIV data. Further investigations are planned using synthetically generated PIV images, in particular to improve the estimation of the fluctuating displacement (velocity) components through analysis of the ensemble-averaged correlation plane.

References

[1] Wereley S, Meinhart C, Santiago J, Beebe D, Adrian R (1998) A micro particle image velocimetry system. *Exp.Fluids* **25**: 316-319
[2] Westerweel J, Geelhoed PF, Lindken R (2004) Single pixel resolution ensemble correlation for micro-PIV applications. *Exp Fluids* **37**: 375-384
[3] Kähler C, Scholz U (2006) Transonic jet analysis using long-distance micro-PIV. *Proc. 12th Intl. Symp. On Flow Visualization*, 10-14 Sep. 2006, Göttingen (Germany)
[4] Hohreiter V, Wereley ST, Olsen MG, Chung JN (2002) Cross-correlation analysis for temperature measurement. *Meas. Sci. Technol.* **13**: 1072-1078
[5] Hart D P (2000) PIV error correction. *Exp Fluids* **29**: 13-22
[6] Westerweel J, Dabiri D & Gharib M (1997) The effect of a discrete window offset on the accuracy of cross-correlation analysis of digital PIV recordings. *Exp. Fluids* **23**: 20-28
[7] Willert C (1997) Stereoscopic digital particle image velocimetry for application in wind tunnel flows. *Meas. Sci. Technol.* **8** 1465-1479
[8] Adrian R (1988) Statistical properties of particle image velocimetry measurements in turbulent flow. *Laser Anemometry in Fluid Mechanics* ed. RJ Adrian et al. (Lisbon: Instituto Superior Tecnico) pp. 115-129
[9] Westerweel J (1997) Fundamentals of digital particle image velocimetry. *Meas Sci Technol* **8**: 1379-1392
[10] Garbov B S, Hillstrom K E, More J J (1980) Public domain library netlib:minpack, *Argonne National Laboratories*
[11] Voges M, Schnell R, Willert C, Moenig R, Mueller M W, Zscherp C (2008) Investigation of blade tip interaction with casing treatment in a transonic compressor – Part 1: particle image velocimetry *Proc. ASME Turbo-Expo, Berlin*, GT2008 – 50210
[12] Schnell R, Voges M, Moenig R, Mueller M W, Zscherp C (2008) Investigation of blade tip interaction with casing treatment in a transonic compressor – Part 2: numerical results *Proc. ASME Turbo-Expo, Berlin*, GT2008 – 50212
[13] Voges M, Willert C, Schnell R, Müller MW, Zscherp C (2008) PIV application for investigation of the rotor blade tip interaction with a casing treatment in a transonic compressor stage. *14th Intern. Symp. on Laser Applications to Fluid Mechanics*, Lisbon, 07-10 July 2008
[14] Kallweit S, Willert C, Dues M, Müller U, Lederer T (2008) PIV for volume flow metering. *14th Intern. Symp. on Laser Applications to Fluid Mechanics*, Lisbon, 07-10 July 2008

Appendix

A.1 Optimized FFT-based cross-correlation

For reasons of efficiency the calculation of the two-dimensional cross-correlation is generally performed via the fast Fourier transform (FFT) which reduces the operation to a complex-conjugate multiplication of the respective Fourier coefficients. The ensemble correlation method, relying on the summation of correlation planes, can be made more efficient by exploiting the summation property of Fourier transform: For two functions $x(t)$ and $y(t)$ with corresponding Fourier transforms $F[x(t)]$ and $G[y(t)]$ the transform of the sum of the functions is equivalent to summing the Fourier coefficients.

$$F_k\left[x(t)\right]+G_k\left[y(t)\right]=\sum_{j=0}^{N-1}x_j e^{-2\pi i\frac{jk}{N}}+\sum_{j=0}^{N-1}y_j e^{-2\pi i\frac{jk}{N}}=\sum_{j=0}^{N-1}(x_j+y_j)e^{-2\pi i\frac{jk}{N}}=H_k\left[(x_j+y_j)\right]$$

Therefore a summation of the cross-power spectra (the Fourier transform of the cross-correlation) is equivalent to summing the individual cross-correlation planes. As shown in Fig. A1 only one transform at the end of the ensemble averaging procedure is then required to obtain the average cross-correlation plane, which reduces the processing time approximately by one third.

A.2 Peak detection and fitting

Contrary to standard PIV to peak detection and fitting algorithm requires special attention. In

particular the ensemble-averaged correlation peak generally is strongly elliptic and does not have its major axes aligned with the Cartesian observation grid. Therefore a higher order fit is required to retrieve the correlation peak shape. The generalized two-dimensional Gaussian function

$$f(x,y) = C_0 + A\exp\left[-(a(x-x_0)^2 + 2b(x-x_0)(y-y_0) + c(y-y_0)^2\right]$$

describes elliptical Gaussian function oriented in any direction, centered at $[x_o,y_o]$ with a peak amplitude of A. The coefficients a,b,c are related to the width σ_x, σ_y and angle θ of the correlation peak through the expressions:

$$a = \frac{\cos^2(\theta)}{2\sigma_x^2} + \frac{\sin^2(\theta)}{2\sigma_y^2} \qquad b = \frac{-2\sin(2\theta)}{4\sigma_x^2} + \frac{2\sin(2\theta)}{4\sigma_y^2} \qquad c = \frac{\sin^2(\theta)}{2\sigma_x^2} + \frac{\cos^2(\theta)}{2\sigma_y^2}$$

However the non-linear minimization procedure required to extract the 10 parameters is difficult to implement reliably and suffers from slow convergence.
In the present case a slightly modified version of the above expressions was minimized:

$$f(x,y) = C_0 + A\exp\left[-\left(\frac{(x-x_0)^2}{2\sigma_x^2} + \frac{(y-y_0)^2}{2\sigma_y^2} + k(x-x_0)(y-y_0)\right)\right]$$

For a constant $k \equiv 0$ the equation reduces to the conventional two-dimensional Gaussian function of elliptic shape with major axis aligned to the Cartesian grid. Non-zero constants k indicate a rotation in the ellipse and correspond to nonzero Reynolds stresses $u'v'$.

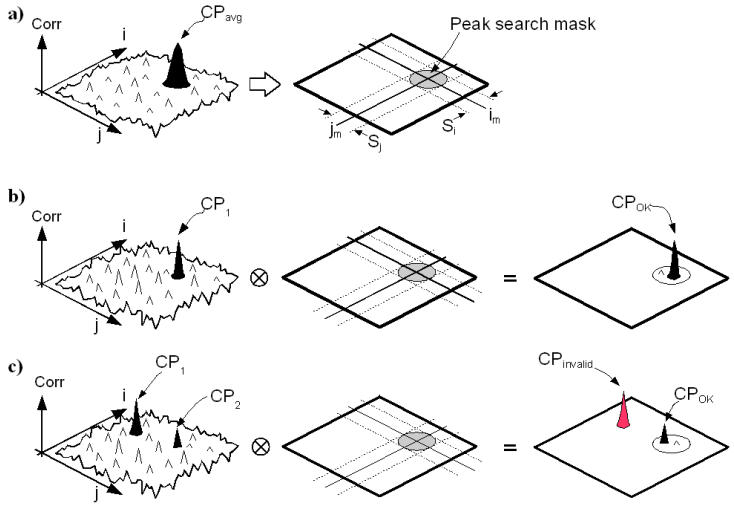

Fig. 6 a) Extraction of correlation peak search mask (SM) from ensemble-correlation data, b) detection of correlation peak (CP) SM, c) recovery of weaker correlation peak from noisy correlation data.

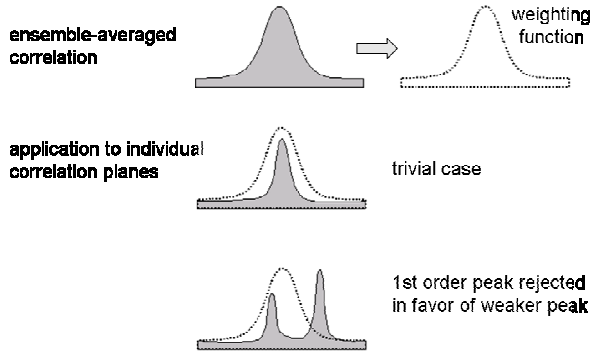

Fig. 7 Use of averaged correlation peak to extract weighting function for recovery of correlation peaks from individual image pairs

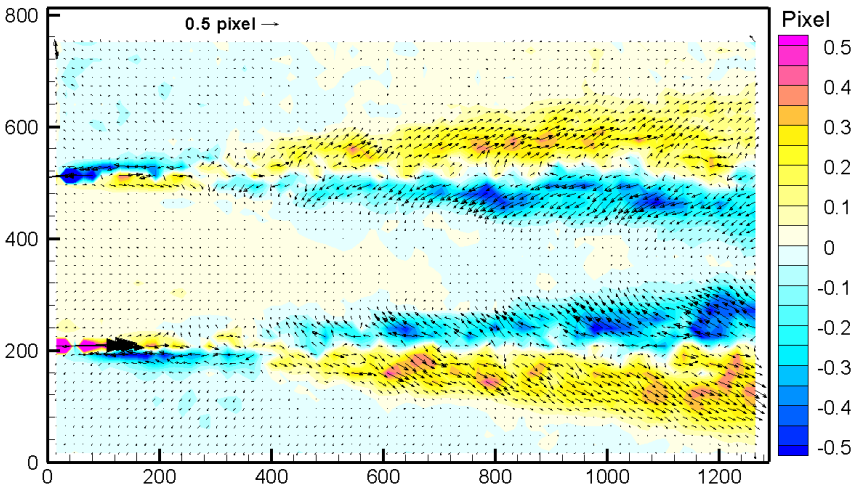

Fig. 8 Map of displacement difference between conventionally averaged PIV data and ensemble correlation PIV data. Contours correspond to the horizontal displacement difference.

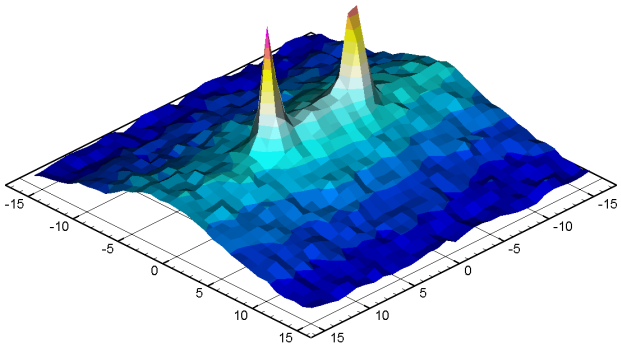

Fig. 9 Average correlation map with tow correlation peaks obtained in the shear layer at the exit of the nozzle.

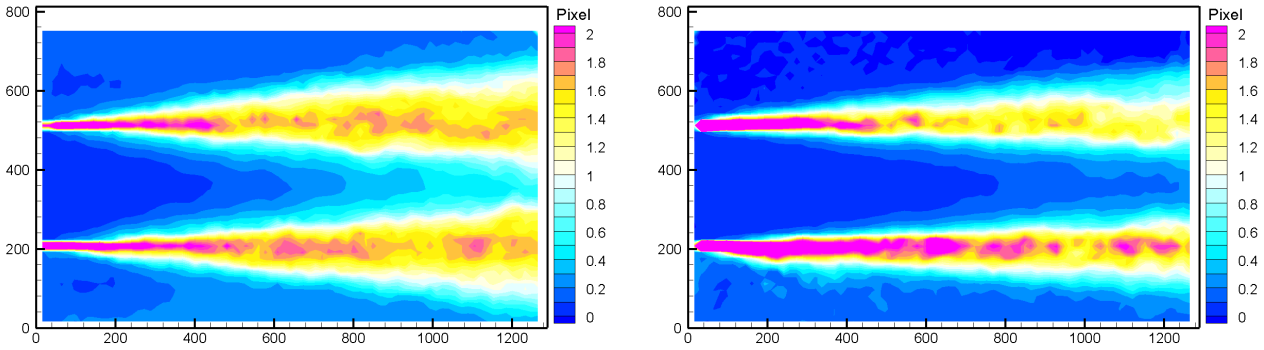

Fig. 10 Estimated root-mean-square values for the horizontal displacement component obtained with standard PIV (left) and proposed ensemble correlation method (right)

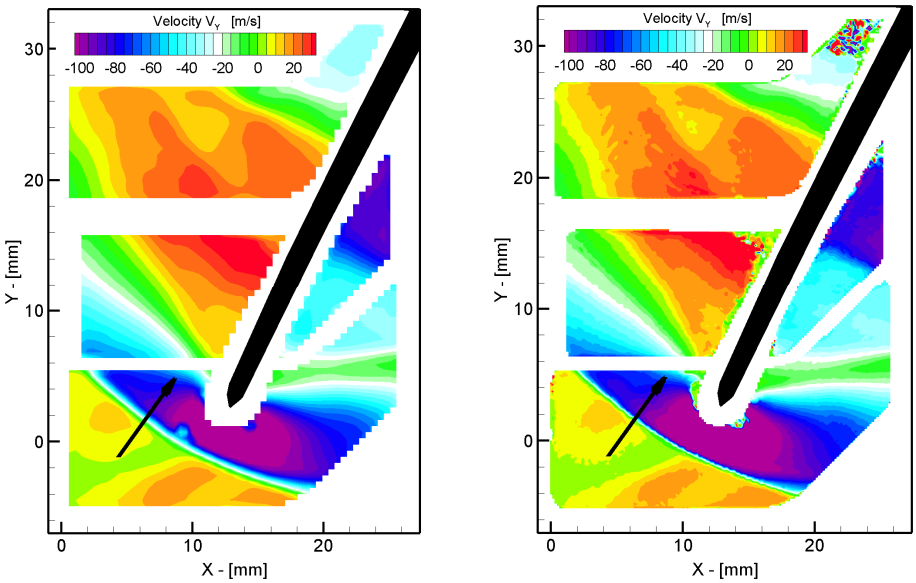

Fig. 11: PIV measurement data of the flow inside a transonic compressor rotor with casing treatment. Left: average velocity field obtained with standard PIV. Right: average velocity field obtained with described ensemble correlation (Flow is from left-to-right, compressor blade is moving vertically from top-to-bottom)

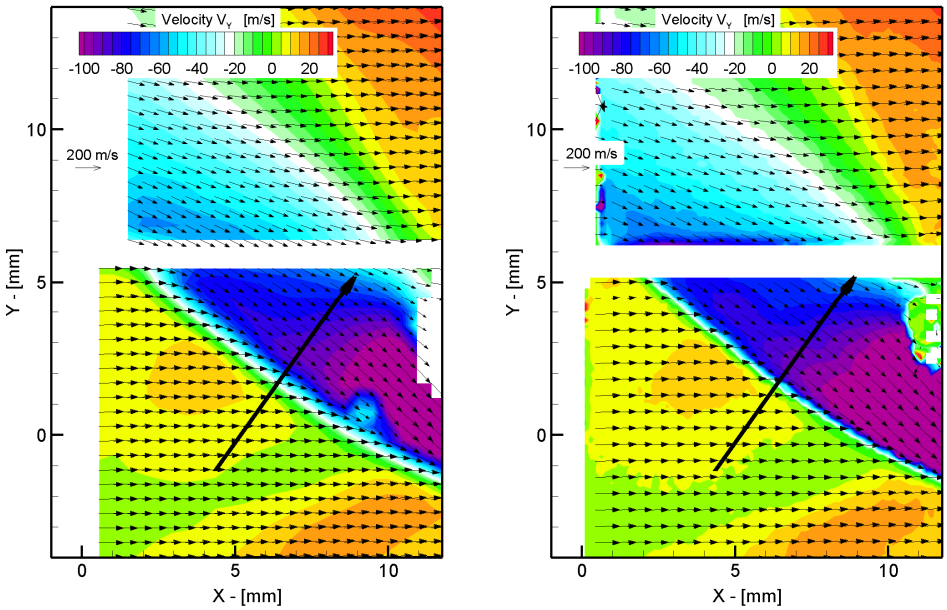

Fig. 12: Detail of Fig. 11 showing the compression shock region upstream of the blade's leading edge: Left: result obtained with standard PIV. Right: ensemble correlation result with only every 9th vector shown. (The line indicates the sampling position for data shown in Fig. 13)

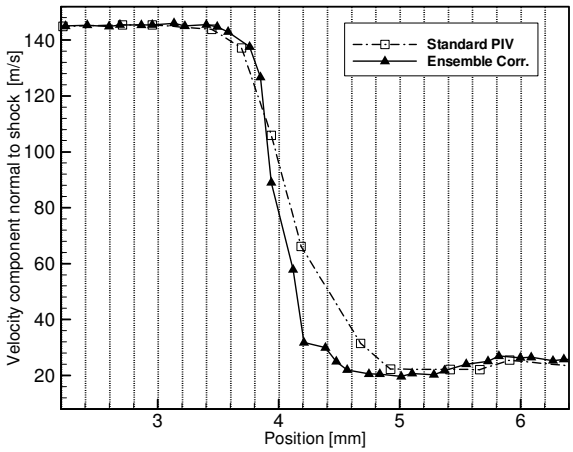

Fig. 13: Plot of velocity component tangential to line shown in Fig. 12

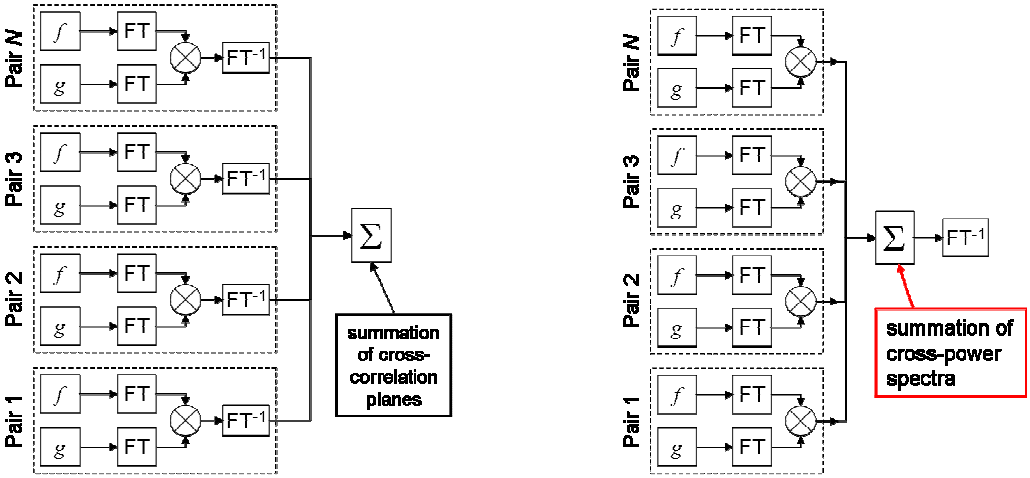

Fig. A1: Increased processing speed can be achieved by summing the cross-power spectra rather than the cross-correlation planes simply by using the summation property of the Fourier transform.